Infrared Spectroscopic and Theoretical Studies on the Reactions of Copper Atoms with Carbon Monoxide and Nitric Oxide Molecules in Rare-Gas Matrices

Ling Jiang and Qiang Xu*

National Institute of Advanced Industrial Science and Technology (AIST), Ikeda, Osaka 563-8577, Japan, and Graduate School of Science and Technology, Kobe University, Nada Ku, Kobe, Hyogo 657-8501, Japan

Received: October 27, 2006; In Final Form: January 30, 2007

Reactions of laser-ablated Cu atoms with CO and NO mixtures in solid argon and neon have been investigated using matrix-isolation infrared spectroscopy. Copper carbonyls and copper nitrosyls have been observed, whereas copper carbonyl nitrosyl complexes are absent from the present experiments. New products, $(CuCO)_2$, [NO]Cu[NO], $Cu_2(\mu_2\text{-NO})$, and $Cu(NO)_2Cu$, have been formed in the copper experiments and characterized using infrared spectroscopy on the basis of the results of the isotopic shifts, mixed isotopic splitting patterns, stepwise annealing, the change of reagent concentration and laser energy, and comparison with theoretical predictions. Density functional theory calculations have been performed on these copper carbonyls and copper nitrosyls, which support the identification of these products from the matrix infrared spectrum. A plausible reaction mechanism has been proposed to account for the formation of copper carbonyls and copper nitrosyls. Similar matrix experiments with Ag and Au produce no new species.

Introduction

The interaction of transition metal centers with carbon monoxide and nitric oxide is of considerable interest from an academic or an industrial viewpoint.[1−3] Many industrial processes employ CO as a reagent and transition metal compounds as heterogeneous catalysts and involve the intermediates of metal carbonyls. For instance, metal polycarbonyl cations have been used to catalyze the carbonylation reactions of olefins, alcohols, and saturated hydrocarbons.[4] The so-called "low-temperature" Cu/ZnO catalyst is widely used to catalyze the water-gas shift reaction ($CO + H_2O \rightarrow CO_2 + H_2$), and metallic Cu provides the active site for catalysis; in the surface redox mechanism, CO reacts with an adsorbed oxygen atom to produce CO_2.[5] On the other hand, the reaction of nitric oxide on metal surfaces and in contact with metal cations in zeolites is important in the development of effective catalysts that can reduce atmospheric pollution.[3] Copper-exchanged zeolites have high activities in the catalytic reduction of NO, and considerable experimental and theoretical work has been done to understand the reduction mechanisms.[6] Furthermore, the study of reduction of NO by CO on several metal surfaces has been achieved through molecular beams in conjunction with mass spectrometry and in situ infrared spectroscopy coupled with temperature-programmed reaction techniques.[7] Recently, a series of metal carbonyl nitrosyl complexes have been observed in the matrix investigations of the reactions of manganese, iron, and cobalt atoms with NO and CO mixtures.[8−10]

Recent studies have shown that, with the aid of isotopic substitution, matrix isolation infrared spectroscopy combined with quantum chemical calculations is a powerful technique for investigating the spectrum, structure and bonding of novel species.[11,12] For instance, argon and neon matrix investigations of the reaction of Cu atoms with CO molecules have characterized a series of copper carbonyls, $Cu(CO)_n$ ($n = 1-3$), $Cu_2(CO)_6$, $Cu(CO)_{1-4}^+$, and $Cu(CO)_{1-3}^-$.[13] Similarly, the $Cu(NO)_n$ ($n = 1, 2$), $CuNO^+$, and $Cu(NO)_2^-$ molecules have been identified from isotopic shifts and splitting patterns in the rare-gas matrix infrared spectra.[14] Here, we report a study of the reactions of laser-ablated Cu, Ag, and Au atoms with CO/NO mixtures in excess neon and argon. IR spectroscopy coupled with theoretical calculations provides evidence for the formation of new products, $(CuCO)_2$, [NO]Cu[NO], $Cu_2(\mu_2\text{-NO})$, and $Cu(NO)_2Cu$, with the absence of metal carbonyl nitrosyl complexes.

Experimental and Theoretical Methods

The experiment for laser ablation and matrix isolation infrared spectroscopy is similar to those previously reported.[15,16] Briefly, the Nd:YAG laser fundamental (1064 nm, 10 Hz repetition rate with 10 ns pulse width) was focused on the rotating Cu, Ag, and Au targets. The laser-ablated Cu, Ag, and Au atoms were co-deposited with CO/NO mixtures in excess neon (or argon) onto a CsI window cooled normally to 4 K (or 7 K) by means of a closed-cycle helium refrigerator. Typically, 1−20 mJ pulse^{-1} laser pulse energies were used. CO (99.95%, Japan Fine Products Co.), $^{13}C^{16}O$ (99%, $^{18}O < 1\%$, ICON), $^{12}C^{18}O$ (^{18}O enrichment 99%, ICON), NO (99.8%, Sumitomo Seika), $^{15}N^{16}O$ (^{15}N enrichment 99%, SHOKO Co. Ltd.), and $^{14}N^{18}O$ (^{18}O enrichment 93%, SHOKO Co. Ltd.) were used to prepare the CO + NO/Ne (or CO + NO/Ar) mixtures. In general, matrix samples were deposited for 30−60 min with a typical rate of 2−4 mmol per hour. After sample deposition, IR spectra were recorded on a BIO-RAD FTS-6000e spectrometer at 0.5 cm^{-1} resolution using a liquid nitrogen cooled HgCdTe (MCT) detector for the spectral range of 5000−400 cm^{-1}. Samples were annealed at different temperatures and subjected to broad-band irradiation ($\lambda > 250$ nm) using a high-pressure mercury arc lamp (Ushio, 100 W). Experiments have also been conducted for the co-deposition of laser-ablated Cu, Ag, and Au atoms with separated CO and NO samples to confirm the new absorptions.

* Corresponding author. E-mail: q.xu@aist.go.jp.

10.1021/jp067050w CCC: $37.00
Published on Web 03/22/2007

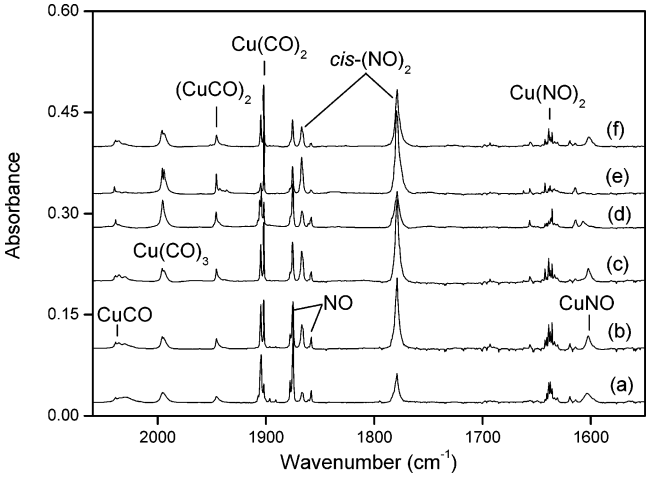

Figure 1. Infrared spectra in the 2050−1600 cm^{-1} region from co-deposition of laser-ablated (18 mJ $pulse^{-1}$) Cu atoms with 0.2% CO + 0.2% NO in Ne: (a) 30 min of sample deposition at 4 K; (b) after annealing to 8 K; (c) after annealing to 10 K; (d) after 15 min of broad-band irradiation; (e) after annealing to 11 K; (f) 0.2% CO + 0.2% NO + 0.05% CCl_4, after annealing to 10 K.

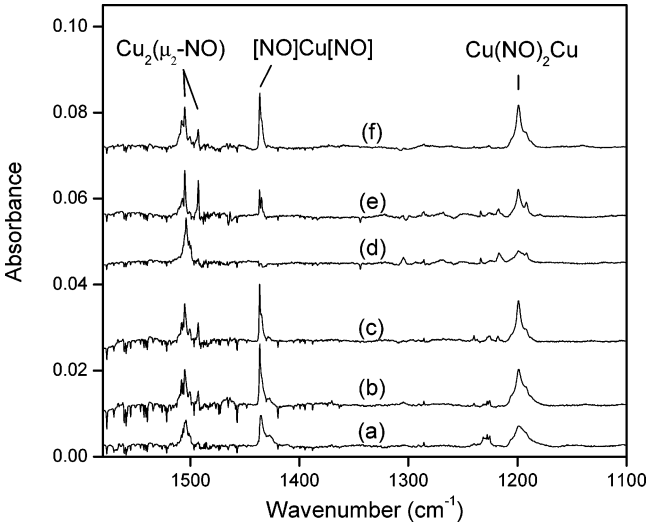

Figure 2. Infrared spectra in the 1550−1100 cm^{-1} region from co-deposition of laser-ablated (18 mJ $pulse^{-1}$) Cu atoms with 0.2% CO + 0.2% NO in Ne: (a) 30 min of sample deposition at 4 K; (b) after annealing to 8 K; (c) after annealing to 10 K; (d) after 15 min of broad-band irradiation; (e) after annealing to 11 K; (f) 0.2% CO + 0.2% NO + 0.05% CCl_4, after annealing to 10 K.

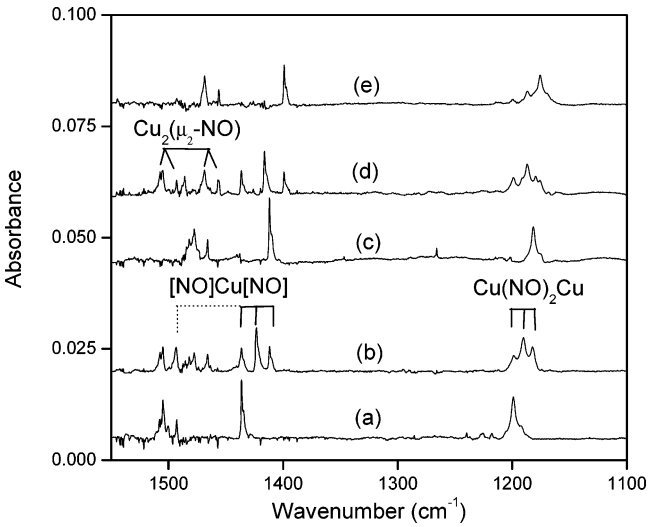

Figure 3. Infrared spectra in the 1550−1100 cm^{-1} region from co-deposition of laser-ablated (18 mJ $pulse^{-1}$) Cu atoms with isotopic CO/NO mixtures in Ne after annealing to 10 K: (a) 0.2% $^{12}C^{16}O$ + 0.2% $^{14}N^{16}O$; (b) 0.3% $^{12}C^{16}O$ + 0.2% $^{14}N^{16}O$ + 0.2% $^{15}N^{16}O$; (c) 0.2% $^{12}C^{16}O$ + 0.2% $^{15}N^{16}O$; (d) 0.3% $^{12}C^{16}O$ + 0.2% $^{14}N^{16}O$ + 0.2% $^{14}N^{18}O$; (e) 0.2% $^{12}C^{16}O$ + 0.2% $^{14}N^{18}$.

Quantum chemical calculations were performed to predict the structures and vibrational frequencies of the observed reaction products using the Gaussian 03 program.[17] The BP86 and B3LYP density functional methods were used.[18] The 6-311+G(d) was used for C, N, and O atoms,[19] the Wachters-Hay all-electron basis set for Cu and the LANL2DZ basis set for Ag and Au.[20] Geometries were fully optimized and vibrational frequencies were calculated with analytical second derivatives. Transition-state optimizations were done with the QST3 algorithm within the synchronous transit-guided quasi-Newton (STQN) method, followed by the vibtrational calculations showing the obtained structures to be true saddle points. The intrinsic reaction coordinate (IRC) method was used to track minimum energy paths from transition structures to the corresponding local minima. A step size of 0.1 $amu^{1/2}$ bohr was used in the IRC procedure. The previous investigations have shown that such computational methods can provide reliable information for metal carbonyls and metal nitrosyls, such as infrared frequencies, relative absorption intensities, and isotopic shifts.[2]

Results and Discussion

Experiments have been done with CO and NO concentrations ranging from 0.01% to 1.0% in excess neon and argon. New absorptions have been observed in the copper experiments but not in the silver and gold experiments. Here, mainly the results from the reactions of Cu with CO and NO will be presented for discussion. Typical infrared spectra for the reactions of laser-ablated Cu atoms with CO and CO/NO mixtures in excess neon in the selected regions are illustrated in Figures 1−6, and the absorption bands in different isotopic experiments are listed in Table 1. Metal independent absorptions due to the $(NO)_2$, $(NO)_2^+$, $(NO)_2^-$, NO_2, NO^-, $(NO)_3^-$, and N_2O_3 species have been reported previously[21−24] and are not listed here. The stepwise annealing and photolysis behavior of the product absorptions are also shown in the figures and will be discussed below. Experiments were also done with different concentrations of CCl_4 serving as an electron scavenger.

Quantum chemical calculations have been carried out for the possible isomers and electronic states of the potential product molecules. Figure 7 shows the optimized structures of the reaction products. Calculated C−O and N−O stretching modes with different functional methods have been compared with the experimental values in Tables 2 and 3, respectively.

$Cu(CO)_n$ (n = 1−3) and $Cu(NO)_n$ (n = 1, 2). The absorptions at 2038.7, 2035.1, and 2029.0 cm^{-1} (Table 1 and Figures 1 and 4) are due to the C−O stretching vibration of the CuCO molecule, which is consistent with the previous reports of 2034.9 and 2029.7 cm^{-1} absorptions.[13c] The 1904.9, 1902.0, and 1995.5 cm^{-1} bands (Table 1 and Figures 1 and 4) are due to the antisymmetric C−O stretching vibrations of the $Cu(CO)_2$ and $Cu(CO)_3$ molecules, respectively. The absorptions at 1602.5 and 1635.9 cm^{-1} (Table 1 and Figure 1) are due to the N−O stretching vibrations of the CuNO and $Cu(NO)_2$ molecules, respectively. Detailed discussions about these copper carbonyls and copper nitrosyls have been reported previously[13,14] and we will focus on the new reaction products.

$(CuCO)_2$. In the Cu + CO experiment, the absorption at 1946.0 cm^{-1} that appears during sample deposition increases

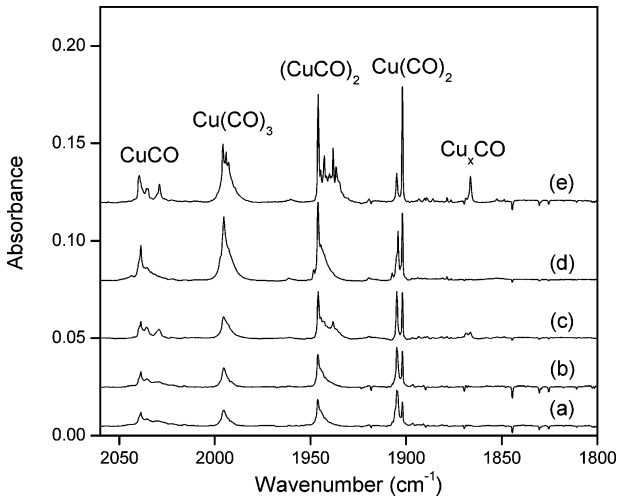

Figure 4. Infrared spectra in the 2050−1800 cm^{-1} region from co-deposition of laser-ablated (15 mJ $pulse^{-1}$) Cu atoms with 0.05% CO in Ne: (a) 30 min of sample deposition at 4 K; (b) after annealing to 8 K; (c) after annealing to 10 K; (d) after 15 min of broad-band irradiation; (e) after annealing to 11 K.

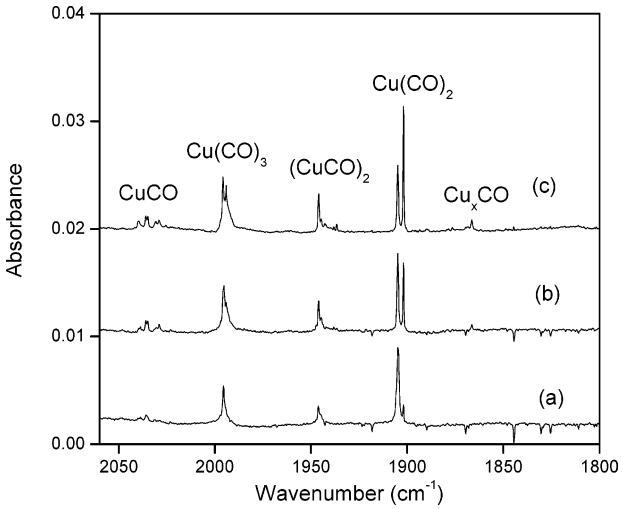

Figure 5. Infrared spectra in the 2050−1800 cm^{-1} region from co-deposition of laser-ablated (8 mJ $pulse^{-1}$) Cu atoms with 0.2% CO in Ne: (a) 30 min of sample deposition at 4 K; (b) after annealing to 10 K; (c) after annealing to 11 K.

slightly on sample annealing, increases visibly after broad-band irradiation and increases slightly on further annealing (Figure 4). The 1946.0 cm^{-1} band shifts to 1901.5 cm^{-1} with $^{13}C^{16}O$ and to 1902.8 cm^{-1} with $^{12}C^{18}O$, exhibiting isotopic frequency ratios ($^{12}C^{16}O/^{13}C^{16}O$, 1.0234; $^{12}C^{16}O/^{12}C^{18}O$, 1.0227) characteristic of C−O stretching vibrations (Table 1 and Figure 6). The 1946.0 cm^{-1} band has also been observed in the Cu + CO + NO experiments (Figure 1) and exhibits no isotopic shifts with $^{15}N^{16}O$ and $^{14}N^{18}O$. This suggests that no NO subunit is involved in this vibration. A triplet at 1946.0, 1918.5, and 1901.5 cm^{-1}, together with a weak associated band at 2022.1 cm^{-1}, has been observed in the mixed $^{12}C^{16}O + ^{13}C^{16}O$ experiment (Figure 6, trace b), indicating that two CO subunits are involved.[25] A similar isotopic splitting feature has been obtained in the mixed $^{12}C^{16}O + ^{12}C^{18}O$ isotopic spectra (Figure 6, trace d). The IR spectra as a function of changes of CO concentrations and laser powers are of particular interest here. The $Cu(CO)_n$ ($n = 1-3$) molecules are the primary products under the experimental conditions of high CO concentration (0.2%) and low laser power (8 mJ $pulse^{-1}$) (Figure 5), whereas the intensity

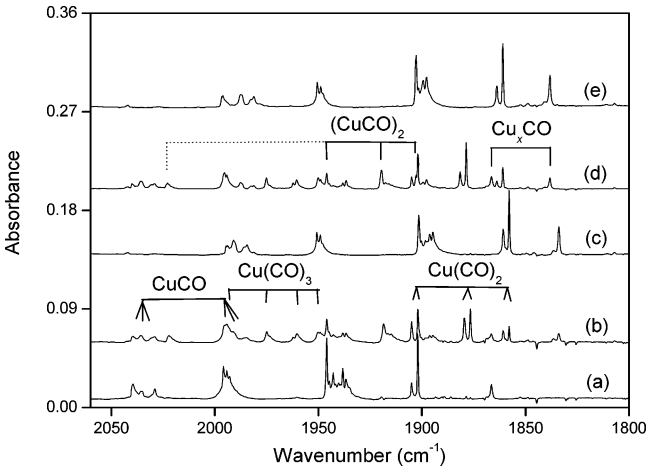

Figure 6. Infrared spectra in the 2050−1800 cm^{-1} region from co-deposition of laser-ablated (15 mJ $pulse^{-1}$) Cu atoms with isotopic CO in Ne after 15 min of broad-band irradiation and annealing to 11 K: (a) 0.05% $^{12}C^{16}O$; (b) 0.03% $^{12}C^{16}O$ + 0.03% $^{13}C^{16}O$; (c) 0.05% $^{13}C^{16}O$; (d) 0.03% $^{12}C^{16}O$ + 0.03% $^{12}C^{18}O$; (e) 0.05% $^{12}C^{18}O$.

of the 1946.0 cm^{-1} band increases greatly under the experimental conditions of lower CO concentration (0.05%) and higher laser power (15 mJ $pulse^{-1}$) (Figure 4). Considering that the experimental conditions of higher CO concentration and lower laser energy favor the formation of the mononuclear metal carbonyls whereas the experimental conditions of lower CO concentration and higher laser energy favor the formation of the polynuclear metal carbonyls,[26,27] this new absorption (1946.0 cm^{-1}) should involve more than one Cu atom. Doping with CCl_4 has no effect on this band (Figure 1, trace f), suggesting that the product is neutral.[2] Furthermore, N_2- or H_2O-doping exhibits no effect on the absorption at 1946.0 cm^{-1} (not shown here), indicating that N_2 and H_2O are not involved in the formation of this species. Accordingly, the 1946.0 cm^{-1} band is assigned to the antisymmetric C−O stretching mode of $(CuCO)_2$. The bands observed at 2022.1 cm^{-1} in the mixed $^{12}C^{16}O + ^{13}C^{16}O$ experiment and 2021.9 cm^{-1} in the $^{12}C^{16}O + ^{12}C^{18}O$ experiment are due to the symmetric C−O stretching modes of $(Cu^{12}CO)$-$(Cu^{13}CO)$ and $(CuC^{16}O)(CuC^{18}O)$, respectively. Analogous molecular structures have been obtained from $(MCO)_2$ (M═Ag, Au; Si, Ge, Sn) spectra.[26,27]

Density functional theory (DFT) calculations have been performed to support the $(CuCO)_2$ assignment. At the BP86/6-311+G(d) and B3LYP/6-311+G(d) levels, the $(CuCO)_2$ molecule is predicted to have C_{2h} symmetry with an ^1A_g ground electronic state (Table 2 and Figure 7), which lies 38 kcal mol^{-1} lower in energy than the triplet state. The calculated $^{12}C^{16}O/^{13}C^{16}O$ and $^{12}C^{16}O/^{12}C^{18}O$ isotopic frequency ratios of 1.0240 and 1.0228 (BP86), 1.0236 and 1.0235 (B3LYP) are in agreement with the experimental observations, 1.0234 and 1.0227, respectively. Both functionals predict that the singlet and triplet $CuCu(CO)_2$ isomers with C_{2v} symmetry are about 2 and 28 kcal mol^{-1} higher in energy than singlet $(CuCO)_2$, respectively. At the BP86/6-311+G(d) level, the symmetric and antisymmetric C−O stretching frequencies in the singlet $CuCu(CO)_2$ isomer are calculated at 2048.7 (480) and 2013.8 (1383 km/mol) cm^{-1}, showing $^{12}C^{16}O/^{13}C^{16}O$ and $^{12}C^{16}O/^{12}C^{18}O$ isotopic frequency ratios of 1.0240 and 1.0236, 1.0230 and 1.0236, respectively. Considering that the $CuCu(CO)_2$ isomer needs two sets of triplet patterns while only one set of triplet pattern with a weak associated band has been observed for the 1946.0 cm^{-1} band in the mixed $^{12}C^{16}O + ^{13}C^{16}O$ and $^{12}C^{16}O + ^{12}C^{18}O$ isotopic spectra (Figure 6, traces b and d),

TABLE 1: Infrared Absorptions (cm^{-1}) Observed for the Copper Carbonyls and Nitrosyls in Excess Neon at 4 K

$^{12}C^{16}O$	$^{13}C^{16}O$	$^{12}C^{18}O$	$^{12}C^{16}O + ^{13}C^{16}O$	$^{12}C^{16}O + ^{12}C^{18}O$	R(12/13)	R(16/18)	assignment
2038.7	1994.2	1990.7	2038.7, 1994.2	2038.7, 1990.7	1.0223	1.0241	CuCO
2035.1	1991.0	1987.4	2035.1, 1991.0	2035.1, 1987.4	1.0221	1.0240	CuCO site
2029.0	1984.5	1981.2	2029.0, 1984.5	2029.0, 1981.2	1.0224	1.0241	CuCO site
1995.5	1950.3	1950.1	1995.5, 1975.1, 1960.3, 1950.1	1995.3, 1975.3, 1961.5, 1950.1	1.0232	1.0233	$Cu(CO)_3$
1946.0	1901.5	1902.8	1946.0, 1918.5, 1901.5, 2022.1 (sym)	1946.0, 1919.6, 1902.0, 2021.9 (sym)	1.0234	1.0227	$(CuCO)_2$
1904.9	1860.7	1863.8	1904.9, 1879.5, 1860.7	1904.9, 1881.5, 1863.8	1.0238	1.0221	$Cu(CO)_2$ site
1902.0	1857.9	1860.9	1901.9, 1876.6, 1857.9	1902.0, 1878.6, 1860.9	1.0237	1.0221	$Cu(CO)_2$
1866.4	1833.8	1838.2	1866.5, 1833.9	1866.4, 1838.2	1.0178	1.0153	Cu_xCO
$^{14}N^{16}O$	$^{15}N^{16}O$	$^{14}N^{18}O$	$^{14}N^{16}O + ^{15}N^{16}O$	$^{14}N^{16}O + ^{14}N^{18}O$	R(14/15)	R(16/18)	
1635.9	1606.5	1605.3	1635.9, 1619.6, 1606.5	1635.9, 1618.7, 1605.3	1.0183	1.0191	$Cu(NO)_2$
1602.5	1574.9	1559.2	1602.5, 1574.9	1602.5, 1559.2	1.0175	1.0278	CuNO
1503.7	1476.3	1468.6	1503.7, 1476.3	1503.7, 1468.6	1.0186	1.0239	$Cu_2(\mu_2\text{-NO})$
1492.7	1465.8	1458.1	1492.7, 1465.8	1492.7, 1458.1	1.0184	1.0237	$Cu_2(\mu_2\text{-NO})$ site
1436.4	1411.8	1399.1	1436.4, 1423.4, 1411.8, 1493.4 (sym)	1436.5, 1416.2, 1399.2, 1486.0 (sym)	1.0174	1.0267	[NO]Cu[NO]
1199.1	1181.7	1175.7	1198.9, 1190.3, 1182.3	1199.3, 1186.9, 1176.0	1.0147	1.0199	$Cu(NO)_2Cu$

TABLE 2: Comparison of Experimental and Calculated C−O Stretching Modes of the Copper Carbonyls

		observed			calculated			
species	mode	freq	$^{12}C/^{13}C$	$^{16}O/^{18}O$	method	freq	$^{12}C/^{13}C$	$^{16}O/^{18}O$
CuCO	a′	2038.7	1.0223	1.0241	BP86	1959.4	1.0230	1.0244
($^2A'$, C_s)					B3LYP	2036.8	1.0227	1.0250
$Cu(CO)_2$	σ_u	1902.0	1.0237	1.0221	BP86	1954.0	1.0242	1.0226
($^2\Pi_u$, $D_{\infty h}$)					B3LYP	1999.1	1.0241	1.0228
$Cu(CO)_3$	e′	1995.5	1.0232	1.0233	BP86	1986.1	1.0238	1.0231
($^3A_2''$, D_{3h})					B3LYP	2050.2	1.0235	1.0237
$(CuCO)_2$	b_u	1946.0	1.0234	1.0227	BP86	2031.4	1.0234	1.0239
(^1A_g, C_{2h})					B3LYP	2142.3	1.0231	1.0243

respectively, the $CuCu(CO)_2$ structural isomer should be ruled out. Recent studies indicate that, in most cases, the BP86 functional gives calculated ν_{C-O} and ν_{N-O} frequencies much closer to the experimental values than the B3LYP functional.[2,3,13,14] Hereafter, mainly BP86 results are presented for discussions.

[NO]Cu[NO]. In the Cu + CO + NO experiment, the absorption at 1436.4 cm^{-1} that appears during sample deposition increases markedly upon annealing, disappears after broad-band irradiation, and recovers slightly after further annealing to 11 K (Table 1 and Figure 2). This band shifts to 1411.8 cm^{-1} with $^{15}N^{16}O$ and to 1399.1 cm^{-1} with $^{14}N^{18}O$, exhibiting isotopic frequency ratios ($^{14}N^{16}O/^{15}N^{16}O$, 1.0174; $^{14}N^{16}O/^{14}N^{18}O$, 1.0267) characteristic of N−O stretching vibrations.[3] The 1436.4 cm^{-1} band exhibits no isotopic shifts with $^{13}C^{16}O$ and $^{12}C^{18}O$, suggesting that no CO subunit is involved in this vibration. As shown in Figure 3, a triplet at 1436.4, 1423.4, and 1411.8 cm^{-1} together with a associated band at 1493.4 cm^{-1} has been observed in the mixed CO + $^{14}N^{16}O$ + $^{15}N^{16}O$ experiment, suggesting that two NO subunits are involved.[25] A similar isotopic splitting feature has been obtained in the mixed CO + $^{14}N^{16}O$ + $^{14}N^{18}O$ isotopic spectra (Figure 3). Doping with CCl_4 has no effect on these bands (Figure 1, trace f), suggesting that the product is neutral.[2] The 1436.4 cm^{-1} band is therefore assigned to the N−O stretching vibration of the side-bonded dinitrosyl [NO]Cu[NO]. The absorptions assigned to the [NO]Cu[NO] molecule were not observed in the previous Cu + NO experiments.[14]

The [NO]Cu[NO] molecule is predicted to have C_{2h} symmetry with an ^2A_u ground electronic state (Table 3 and Figure 7), which lies 31 kcal mol^{-1} (BP86) higher in energy than the linear $^2\Pi_u$ isomer, $Cu(NO)_2$. The activation energy for the isomerization of [NO]Cu[NO] to $Cu(NO)_2$ is calculated to be 273 kcal mol^{-1}. Presumably, this large activation barrier prevents isomerization and both species can be observed in rare-gas matrix isolation studies. Interestingly, the [NO]Cu[NO] molecule is only observed in the Cu + CO + NO experiments and not in the Cu + NO experiments, whereas the $Cu(NO)_2$ molecule is observed in both matrix experiments. This suggests that the presence of CO allows this high-energy structural isomer of [NO]Cu[NO] to be formed in the Cu + CO + NO experiments. The calculated ν_{N-O} value (1280.2 cm^{-1}, Table 3) of the doublet [NO]Cu[NO] is quite lower than the observed value (1436.4 cm^{-1}). However, the calculated $^{14}N^{16}O/^{15}N^{16}O$ and

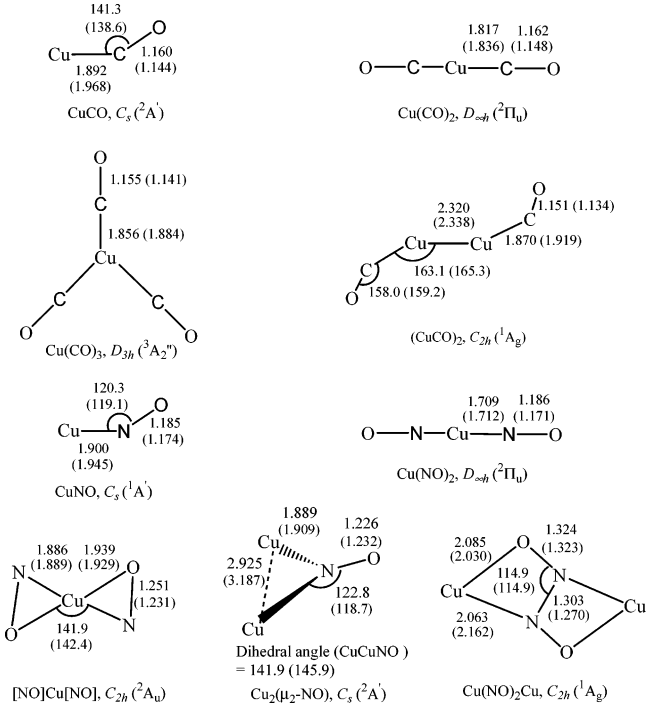

Figure 7. Optimized structures (bond length in angstrom, bond angle in degree) of the reaction products calculated at the BP86 and B3LYP (in parentheses) levels.

TABLE 3: Comparison of Experimental and Calculated N−O Stretching Modes of the Copper Nitrosyls

		observed			calculated			
species	mode	freq	$^{14}N/^{15}N$	$^{16}O/^{18}O$	method	freq	$^{14}N/^{15}N$	$^{16}O/^{18}O$
CuCO ($^1A'$, C_s)	a′	1602.5	1.0175	1.0278	BP86	1652.0	1.0179	1.0276
					B3LYP	1703.6	1.0179	1.0276
$Cu(NO)_2$ ($^2\Pi_u$, $D_{\infty h}$)	σ_u	1635.9	1.0183	1.0191	BP86	1738.0	1.0208	1.0221
					B3LYP	1797.4	1.0206	1.0226
[NO]Cu[No] (^2A_u, C_{2h})	b_u	1436.4	1.0174	1.0267	BP86	1280.2	1.0176	1.0273
					B3LYP	1388.6	1.0183	1.0265
$Cu_2(\mu_2$-NO) ($^2A'$, C_s)	a′	1503.7	1.0186	1.0239	BP86	1416.6	1.0176	1.0280
					B3LYP	1345.1	1.0172	1.0288
$Cu(NO)_2Cu$ (^1A_g, C_{2h})	b_u	1199.1	1.0147	1.0199	BP86	1067.1	1.0179	1.0272
					B3LYP	1077.9	1.0178	1.0277

$^{14}N^{16}O/^{14}N^{18}O$ isotopic frequency ratios of 1.0176 and 1.0273 are in accord with the experimental observations, 1.0174 and 1.0267, respectively.

$Cu_2(\mu_2$-NO). In the Cu + CO + NO experiment, the absorption at 1503.7 cm^{-1} with a matrix trapping site at 1492.7 cm^{-1} is present during sample deposition, increases upon annealing and broad-band irradiation (Table 1 and Figure 2). These two bands respectively shift to 1476.3 and 1465.8 cm^{-1} with $^{15}N^{16}O$ and to 1468.6 and 1458.1 cm^{-1} with $^{14}N^{18}O$, exhibiting isotopic frequency ratios ($^{14}N^{16}O/^{15}N^{16}O$, 1.0186 and 1.0184; $^{14}N^{16}O/^{14}N^{18}O$, 1.0239 and 1.0237) characteristic of N−O stretching vibrations.[3] The 1503.7 and 1492.7 cm^{-1} bands show no isotopic shifts with $^{13}C^{16}O$ and $^{12}C^{18}O$, suggesting that no CO subunit is involved in this vibration. As shown in Figure 3, the mixed CO + $^{14}N^{16}O$ + $^{15}N^{16}O$ and CO + $^{14}N^{16}O$ + $^{14}N^{18}O$ isotopic spectra only provide the sum of pure isotopic bands, which indicates a mononitrosyl molecule.[25] Doping with CCl_4 has no effect on these bands (Figure 2, trace f), implying that the product is neutral.[2] Note that these two bands are observed in the experiments with relatively higher laser power (18 mJ $pulse^{-1}$), which implies that the new product involves more than one copper atom. The 1503.7 and 1492.7 cm^{-1} bands are assigned to the N−O stretching vibration of a species having Cu_2NO stoichiometry in different matrix sites.

BP86 calculations predict that the doublet end-on CuCuNO with $^2A'$ state is 15 kcal mol^{-1} lower in energy than the bridge-bonded Cu−(NO)−Cu isomer, which is in accord with the previous theoretical investigations.[14a,28] The calculated N−O stretching vibrational frequency for the $^2A'$ state end-on CuCuNO (1726.6 cm^{-1}) fits the argon experimental observation (1734.8 cm^{-1})[14a] but does not fit the neon experimental values (1503.7 and 1492.7 cm^{-1}). The $^2A'$ bridge-bonded $Cu_2(\mu_2$-NO) isomer has C_s symmetry (Figure 7), which lies 6 kcal mol^{-1} lower in energy than a quartet state. For the $^2A'$ bridge-bonded $Cu_2(\mu_2$-NO), the N−O stretching vibrational frequency is calculated at 1416.6 cm^{-1} (Table 3). The calculated $^{14}N^{16}O/^{15}N^{16}O$ and $^{14}N^{16}O/^{14}N^{18}O$ isotopic frequency ratios of 1.0176 and 1.0280 (Table 3) are consistent with the experimental observations, 1.0186 and 1.0239, respectively. Accordingly, the 1503.7 and 1492.7 cm^{-1} bands are assigned to the N−O stretching vibration of the bridge-bonded $Cu_2(\mu_2$-NO) complex in solid neon. The argon matrix counterpart has been observed at 1529.3 and 1524.5 cm^{-1} but its structure was not characterized.[14a] The absorptions assigned to the $Cu_2(\mu_2$-NO) molecule were not observed in the previous Cu + NO experiments in solid neon.[14]

$Cu(NO)_2Cu$. In the Cu + CO + NO experiment, the absorption at 1199.1 cm^{-1} appears weakly during sample deposition, increases visibly after sample annealing, decreases sharply after broad-band irradiation, and recovers slightly after further annealing to 11 K (Table 1 and Figure 2). The 1199.1 cm^{-1} band shifts to 1181.7 cm^{-1} with $^{15}N^{16}O$ and to 1175.7 cm^{-1} with $^{14}N^{18}O$, giving the $^{14}N^{16}O/^{15}N^{16}O$ and $^{14}N^{16}O/^{14}N^{18}O$ isotopic frequency ratios of 1.0147 and 1.0199, respectively. This band shows no isotopic shifts with $^{13}C^{16}O$ and $^{12}C^{18}O$, suggesting that no CO subunit is involved in this vibration. Two sets of triplet bands have been observed at 1198.9/1190.3/1182.3 and 1199.3/1186.9/1176.0 cm^{-1} in the mixed CO + $^{14}N^{16}O$ + $^{15}N^{16}O$ and CO + $^{14}N^{16}O$ + $^{14}N^{18}O$ isotopic spectra (Table 1 and Figure 3). Doping with CCl_4 has no effect on this band (Figure 2, trace f), suggesting that the product is neutral.[2] Analogy with $Ag(NO)_2Ag$ with the extremely low N−O stretching frequencies at 1185.5 cm^{-1} in Ne and 1121.1 cm^{-1} in Ar,[29] the 1199.1 cm^{-1} band is assigned to the antisymmetric N−O stretching mode of the $Cu(NO)_2Cu$ molecule. The absorptions assigned to the $Cu(NO)_2Cu$ molecule were not observed in the previous Cu + NO experiments.[14] Similar reactions of laser-ablated Ag and Au atoms with NO and CO/NO mixtures give the analogous silver atom absorptions but not the analogous gold atom absorptions. The isomer $Cu_2(NO)_2$ with D_{2h} symmetry has been observed at 1499.6 cm^{-1} in the neon Cu + NO experiments.[14a]

Our BP86 calculations predict that the $Cu(NO)_2Cu$ molecule has a ^1A_g ground state with C_{2h} symmetry (Figure 7), which lies 35 kcal mol^{-1} lower in energy than the triplet one. The ∠NNO bond angle is 114.9°, which is slightly smaller than that in $Ag(NO)_2Ag$ (118.4° (BPW91) and 117.9° (B3LYP)).[29] The antisymmetric N−O stretching vibrational frequency is calculated at 1067.1 cm^{-1} (Table 3), lower than the experimental value. Employing the LANL2DZ basis set for Cu atom lifts the nitrosyl stretching frequency up to 1093.3 cm^{-1}. For $Ag(NO)_2Ag$, the calculated antisymmetric N−O stretching vibrational frequencies (1145.9 cm^{-1} at the BPW91/ LANL2DZ/ 6-311+G(d) level and 1128.4 cm^{-1} at the B3LYP/LANL2DZ/ 6-311+G(d) level) match the experimental values (Ne, 1185.5 cm^{-1}; Ar, 1121.1 cm^{-1}) well.[29] Quantum chemical calculations for the $Au(NO)_2Au$ species on the BP86/LANL2DZ/6-311+G(d), BPW91/LANL2DZ/6-311+G(d), and B3LYP/ LANL2DZ/6-311+G(d) levels cannot locate the minimum, which is consistent with the absence of $Au(NO)_2Au$ from the previous[30] and present experiments.

Other Absorptions. In the Cu + CO experiment, the absorption at 1866.4 cm^{-1} appears weakly after annealing to 10 K, disappears after broad-band irradiation, and increases sharply after further annealing to 11 K (Table 1, Figure 4). This band is favored by higher laser energy (Figures 4 and 5), indicating that the product may be a polynuclear copper carbonyl. The 1866.4 cm^{-1} band shifts to 1833.8 cm^{-1} with $^{13}C^{16}O$ and to 1838.2 cm^{-1} with $^{12}C^{18}O$, showing $^{12}C^{16}O/^{13}C^{16}O$ and $^{12}C^{16}O/^{12}C^{18}O$ isotopic frequency ratios of 1.0178 and 1.0153, respectively (Table 1). In the mixed $^{12}C^{16}O$ + $^{13}C^{16}O$ and $^{12}C^{16}O$ + $^{12}C^{18}O$ samples, only pure isotopic counterparts

are observed (Figure 6). Doping with CCl_4 has no effect on this band, suggesting that the product is neutral.[2] N_2- or H_2O-doping exhibits no effect on the absorption at 1866.4 cm^{-1} (not shown here), indicating that N_2 and H_2O are not involved in the formation of this species. DFT calculations for the possible isomers and electronic states of the smallest copper cluster carbonyl Cu_2CO do not reproduce the experimental observations. This band is tentatively assigned to Cu_xCO.

Reaction Mechanism. On the basis of the behavior of sample annealing and photolysis, together with the observed species and calculated stable isomers, a plausible reaction mechanism can be proposed as follows. Under the present experimental conditions, only metal carbonyl and metal nitrosyl species have been observed. Taking the copper carbonyls as an example, the $(CuCO)_2$ molecule appears together with the $Cu(CO)_x$ ($x = 1-3$) molecules during sample deposition and increases together after sample annealing and broad-band irradiation, while there is no obvious evidence for the formation of Cu_2CO (Figure 1). This suggests that the $(CuCO)_2$ molecule may be generated by the dimerization of the CuCO molecule or the addition of a Cu atom to the $Cu(CO)_2$ molecule (reactions 4 and 5); the C_{2h} structure of the $(CuCO)_2$ molecule implies that the contribution for the formation of $(CuCO)_2$ from the former is larger than from the latter. Furthermore, reaction 4 (-60 kcal mol^{-1}) is predicted to be more energetically favorable than reaction 5 (-45 kcal mol^{-1}), which supports the above-mentioned analysis:

$$Cu + CO \rightarrow CuCO \quad (\Delta E = -18 \text{ kcal mol}^{-1}, \text{BP86}) \quad (1)$$

$$CuCO + CO \rightarrow Cu(CO)_2 \quad (\Delta E = -32 \text{ kcal mol}^{-1}) \quad (2)$$

$$Cu(CO)_2 + CO \rightarrow Cu(CO)_3 \quad (\Delta E = -25 \text{ kcal mol}^{-1}) \quad (3)$$

$$CuCO + CuCO \rightarrow (CuCO)_2 \quad (\Delta E = -60 \text{ kcal mol}^{-1}) \quad (4)$$

$$Cu + Cu(CO)_2 \rightarrow (CuCO)_2 \quad (\Delta E = -45 \text{ kcal mol}^{-1}) \quad (5)$$

In the Cu + CO + NO experiments, the yields of new products, [NO]Cu[NO], $Cu_2(\mu_2\text{-NO})$, and $Cu(NO)_2Cu$, increase after sample annealing, whereas the $Cu(NO)_x$ ($x = 1, 2$) molecules change little after sample annealing. Meanwhile, the absorptions of $Cu(NO)_2Cu$ increase upon sample annealing at the expense of *trans*-$(NO)_2$ (1760.6 cm^{-1}),[21] suggesting that the $Cu(NO)_2Cu$ molecule is most probably formed via the combination of two Cu atoms with the *trans*-$(NO)_2$ molecule (reaction 12). The reactions of copper atoms with NO molecules are predicted to be exothermic (reactions 6−12), implying that the formation of copper nitrosyls is energetically favorable.

It can be found from the calculated reaction energies that the formation of copper nitrosyls (reactions 6 and 7) is more exothermic than that of copper carbonyls (reactions 1−3). This is expected since one unpaired electron in a π^* orbital in the NO molecule makes it more reactive than other diatomics like CO. A more interesting finding is that the absorptions of the [NO]Cu[NO], $Cu_2(\mu_2\text{-NO})$, and $Cu(NO)_2Cu$ molecules are only observed in the Cu + CO + NO experiments and not in the Cu + NO experiments. Furthermore, there is no evidence for a group of bands that shift together upon isotopic substitution of both CO and NO. This suggests that no mixed species $Cu(CO)_x(NO)_y$ are observed in the present experiments. It seems that CO has a pronounced effect on the formation of these copper nitrosyls during the reactions of copper atoms with CO/NO mixtures. Further investigation is required to address the reason that the presence of CO allows these new nitrosyls to be formed:

$$Cu + NO \rightarrow CuNO \quad (\Delta E = -28 \text{ kcal mol}^{-1}) \quad (6)$$

$$CuNO + NO \rightarrow Cu(NO)_2 \quad (\Delta E = -39 \text{ kcal mol}^{-1}) \quad (7)$$

$$CuNO + NO \rightarrow [NO]Cu[NO] \quad (DE = -9 \text{ kcal mol}^{-1}) \quad (8)$$

$$Cu + CuNO \rightarrow Cu2(\mu_2\text{-NO}) \quad (\Delta E = -29 \text{ kcal mol}^{-1}) \quad (9)$$

$$Cu + Cu \rightarrow Cu_2 \ (\Delta E = -48 \text{ kcal mol}^{-1}) \quad (10)$$

$$Cu2 + NO \rightarrow Cu_2(\mu_2\text{-NO}) \quad (\Delta E = -9 \text{ kcal mol}^{-1}) \quad (11)$$

$$Cu + \textit{trans}\text{-}(NO)_2 + Cu \rightarrow Cu(NO)_2Cu \quad (\Delta E = -73 \text{ kcal mol}^{-1}) \quad (12)$$

It is noted that the reactions of laser-ablated Cu, Ag, and Au atoms with CO and NO mixtures in solid argon and neon produce only metal carbonyls and metal nitrosyls without metal carbonyl nitrosyl complexes. In contrast, manganese, iron, and cobalt carbonyl nitrosyl complexes have been generated in the recent matrix investigations.[8−10]

Conclusions

Laser-ablated copper atoms with carbon monoxide and nitric oxide mixtures in solid argon and neon produce copper carbonyls and copper nitrosyls with the absence of metal carbonyl nitrosyl complexes. Based on the results of the isotopic substitution, stepwise annealing, the change of reagent concentration and laser energy, and comparison with theoretical predictions, new absorptions at 1946.0, 1436.4, 1503.7, and 1199.1 cm^{-1} have been assigned to $(CuCO)_2$, [NO]Cu[NO], $Cu_2(\mu_2\text{-NO})$, and $Cu(NO)_2Cu$, respectively. Density functional theory calculations have been performed on these copper carbonyls and copper nitrosyls, which support the identification of these products from the matrix infrared spectrum. Similar matrix experiments with Ag and Au produce no new products. The present study reveals that it may be difficult for copper, silver, and gold to form metal carbonyl nitrosyl complexes, while metal carbonyls and metals nitrosyl are readily formed from the reactions of metal atoms with CO/NO mixtures. A plausible reaction mechanism has been proposed to account for the formation of metal carbonyls and metal nitrosyls.

Acknowledgment. This work was supported by a Grant-in-Aid for Scientific Research (B) (Grant No. 17350012) from the Ministry of Education, Culture, Sports, Science and Technology (MEXT) of Japan. L.J. thanks the MEXT of Japan and Kobe University for Honors Scholarship.

References and Notes

(1) Cotton, F. A.; Wilkinson, G.; Murillo, C. A.; Bochmann, M. *Advanced Inorganic Chemistry*, 6th ed.; Wiley: New York, 1999. Liu, Z.-P.; Hu, P. *Topics Catal.* **2004**, *28*, 71, and references therein.

(2) Zhou, M. F.; Andrews, L.; Bauschlicher, C. W., Jr. *Chem. Rev.* **2001**, *101*, 1931. Himmel, H. J.; Downs, A. J.; Greene, T. M. *Chem. Rev.* **2002**, *102*, 4191, and references therein.

(3) Andrews, L.; Citra, A. *Chem. Rev.* **2002**, *102*, 885, and references therein.

(4) Xu, Q. *Coord. Chem. Rev.* **2002**, *231*, 83, and references therein.

(5) van Herwijnen, T.; de Jong, W. A. *J. Catal.* **1980**, *63*, 83. Campbell, C. T.; Daube, K. A. *J. Catal.* **1980**, *104*, 109. Nakumura, J.; Campbell, J. M.; Campbell, C. T. *J. Chem. Soc. Faraday Trans.* **1990**, *86*, 2725. Wang, G. C.; Jiang, L.; Cai, Z. S.; Pan, Y. M.; Zhao, X. Z.; Huang, W.; Xie, K. C.; Li, Y. W.; Sun, Y. H.; Zhong, B. *J. Phys. Chem. B* **2003**, *107*, 557.

(6) See, for example: Shelef, M. *Chem. Rev.* **1995**, *95*, 209, and references therein.

(7) Almusaiteer, K. A.; Chung, S. S. C. *J. Phys. Chem. B* **2000**, *104*, 2265. Gopinath, C. S.; Zaera, F. *J. Phys. Chem. B* **2000**, *104*, 3109.

(8) Wang, X. F.; Zhou, M. F.; Andrews, L. *J. Phys. Chem. A* **2000**, *104*, 7964.

(9) Wang, X. F.; Zhou, M. F.; Andrews, L. *J. Phys. Chem. A* **2000**, *104*, 10104.

(10) Wang, X. F.; Andrews, L. *J. Phys. Chem. A* **2001**, *105*, 4403.

(11) See, for example: Xu, C.; Manceron, L.; Perchard, J. P. *J. Chem. Soc., Faraday Trans*. **1993**, *89*, 1291. Bondybey, V. E.; Smith, A. M.; Agreiter, J. *Chem. Rev*. **1996**, *96*, 2113. Fedrigo, S.; Haslett, T. L.; Moskovits, M. *J. Am. Chem. Soc*. **1996**, *118*, 5083. Khriachtchev, L.; Pettersson, M.; Runeberg, N.; Lundell, J.; Rasanen, M. *Nature* **2000**, *406*, 874. Himmel, H. J.; Manceron, L.; Downs, A. J.; Pullumbi, P. *J. Am. Chem. Soc*. **2002**, *124*, 4448. Li, J.; Bursten, B. E.; Liang, B.; Andrews, L. *Science* **2002**, *295*, 2242. Andrews, L.; Wang, X. *Science* **2003**, *299*, 2049.

(12) Zhou, M. F.; Tsumori, N.; Li, Z.; Fan, K.; Andrews, L.; Xu, Q. *J. Am. Chem. Soc*. **2002**, *124*, 12936. Zhou, M. F.; Xu, Q.; Wang, Z.; von Ragué Schleyer, P. *J. Am. Chem. Soc*. **2002**, *124*, 14854. Jiang, L.; Xu, Q. *J. Am. Chem. Soc*. **2005**, *127*, 42. Xu, Q.; Jiang, L.; Tsumori, N. *Angew. Chem., Int. Ed*. **2005**, *44*, 4338. Jiang, L.; Xu, Q. *J. Am. Chem. Soc*. **2005**, *127*, 8906.

(13) (a) Huber, H.; Kunding, E. P.; Moskovits, M.; Ozin, G. A. *J. Am. Chem. Soc*. **1975**, *97*, 2097. (b) Kasai, P. H.; Jones, P. M. *J. Am. Chem. Soc*. **1985**, *107*, 813. (c) Zhou, M. F.; Andrews, L. *J. Chem. Phys.* **1999**, *111*, 4548.

(14) (a) Zhou, M. F.; Andrews, L. *J. Phys. Chem. A* **2000**, *104*, 2618. (b) Krim, L.; Wang, X. F.; Manceron, L.; Andrews, L. *J. Phys. Chem. A* **2005**, *109*, 10264.

(15) Burkholder, T. R.; Andrews, L. *J. Chem. Phys*. **1991**, *95*, 8697.

(16) Zhou, M. F.; Tsumori, N.; Andrews, L.; Xu, Q. *J. Phys. Chem. A* **2003**, *107*, 2458. Jiang, L.; Xu, Q. *J. Chem. Phys.* **2005**, *122*, 034505.

(17) Frisch, M. J.; Trucks, G. W.; Schlegel, H. B.; Scuseria, G. E.; Robb, M. A.; Cheeseman, J. R.; Montgomery, J. A., Jr.; Vreven, T.; Kudin, K. N.; Burant, J. C.; Millam, J. M.; Iyengar, S. S.; Tomasi, J.; Barone, V.; Mennucci, B.; Cossi, M.; Scalmani, G.; Rega, N.; Petersson, G. A.; Nakatsuji, H.; Hada, M.; Ehara, M.; Toyota, K.; Fukuda, R.; Hasegawa, J.; Ishida, M.; Nakajima, T.; Honda, Y.; Kitao, O.; Nakai, H.; Klene, M.; Li, X.; Knox, J. E.; Hratchian, H. P.; Cross, J. B.; Adamo, C.; Jaramillo, J.; Gomperts, R.; Stratmann, R. E.; Yazyev, O.; Austin, A. J.; Cammi, R.; Pomelli, C.; Ochterski, J. W.; Ayala, P. Y.; Morokuma, K.; Voth, G. A.; Salvador, P.; Dannenberg, J. J.; Zakrzewski, V. G.; Dapprich, S.; Daniels, A. D.; Strain, M. C.; Farkas, O.; Malick, D. K.; Rabuck, A. D.; Raghavachari, K.; Foresman, J. B.; Ortiz, J. V.; Cui, Q.; Baboul, A. G.; Clifford, S.; Cioslowski, J.; Stefanov, B. B.; Liu, G.; Liashenko, A.; Piskorz, P.; Komaromi, I.; Martin, R. L.; Fox, D. J.; Keith, T.; Al-Laham, M. A.; Peng, C. Y.; Nanayakkara, A.; Challacombe, M.; Gill, P. M. W.; Johnson, B.; Chen, W.; Wong, M. W.; Gonzalez, C.; Pople, J. A. *Gaussian 03*, revision B.04; Gaussian, Inc.: Pittsburgh, PA, 2003.

(18) Becke, A. D. *Phys. Rev. A* **1988**, *38*, 3098. Perdew, J. P. *Phys. Rev. B* **1986**, *33*, 8822. Lee, C.; Yang, E.; Parr, R. G. *Phys. Rev. B* **1988**, *37*, 785. Becke, A. D. *J. Chem. Phys*. **1993**, *98*, 5648.

(19) McLean, A. D.; Chandler, G. S. *J. Chem. Phys.* **1980**, *72*, 5639. Krishnan, R.; Binkley, J. S.; Seeger, R.; Pople, J. A. *J. Chem. Phys*. **1980**, *72*, 650.

(20) Wachters, A. J. H. *J. Chem. Phys*. **1970**, *52*, 1033. Hay, P. J. *J. Chem. Phys*. **1977**, *66*, 4377. Hay, P. J.; Wadt, W. R. *J. Chem. Phys*. **1985**, *82*, 299.

(21) Jacox, M. E.; Thompson, W. E. *J. Chem. Phys*. **1990**, *93*, 7609.

(22) Andrews, L.; Zhou, M. F.; Willson, S. P.; Kushto, G. P.; Snis, A.; Panas, I. *J. Chem. Phys.* **1998**, *109*, 177 (argon), and references therein.

(23) Lugez, C. L.; Thompson, W. E.; Jacox, M. E.; Snis, A.; Panis, I. *J. Chem. Phys.* **1999**, *110*, 10345 (neon), and references therein.

(24) Andrews, L.; Zhou, M. F. *J. Chem. Phys*. **1999**, *111*, 6036 (neon), and references therein.

(25) Darling, J. H.; Ogden, J. S. *J. Chem. Soc., Dalton Trans*. **1972**, 2496.

(26) Jiang, L.; Xu, Q. *J. Phys. Chem. A* **2005**, *109*, 1026. Jiang, L.; Xu, Q. *J. Phys. Chem. A* **2006**, *110*, 11488.

(27) (a) Zhou, M. F.; Jiang, L.; Xu, Q. *J. Chem. Phys*. **2004**, *121*, 10474. (b) Zhou, M. F.; Jiang, L.; Xu, Q. *J. Phys. Chem. A* **2005**, *109*, 3325. (c) Jiang, L.; Xu, Q. *Bull. Chem. Soc. Jpn.* **2006**, *79*, 857.

(28) Rochefort, A.; Fournier, R. *J. Phys. Chem.* **1996**, *100*, 13506.

(29) Citra, A.; Andrews, L. *J. Phys. Chem. A* **2001**, *105*, 3042.

(30) Citra, A.; Wang, X. F.; Andrews, L. *J. Phys. Chem. A* **2002**, *106*, 3287.